EASI-STRESS

EUROPEAN ACTIVITY FOR STANDARDIZATION OF INDUSTRIAL RESIDUAL STRESS CHARACTERIZATION

H2020 NMBP-35-2020

Grant Agreement Number: 953219

Deliverable Report:

D2.2 Best practice guidelines

This project has received funding from the European Union's Horizon 2020 research and innovation programme under grant agreement No 953219.

Project Deliverable Information Sheet

EASI-STRESS Project	Project Ref. No. 953219	
	Project Title: EASI-STRESS - European Activity for Standardization of Industrial residual STRESS characterization	
	Project Website: www.easi-stress.eu	
	Deliverable No.: D2.2	
	Deliverable Type: Report	
	Dissemination Level: Public	Contractual Delivery Date: 31/12/2021
		Actual Delivery Date: 01/03/2022
	EC Project Officer: Yanaris Ortega Garcia	

Document Control Sheet

Document	Title: Best practices guidelines	
	Version: 1.0	
	Available at:	
	Files:	
Authorship	Written by	Matthew Roy
	Contributors	David Canelo Yubero Manuel Sanchez Poncela Romain Badyka Wen Cui Ranggi Sahmura Ramadhan Mohamed Fares Slim Hanna Leemreize
	Reviewed by	Philip Withers
	Approved	Nikolaj Zangenberg

This project has received funding from the European Union's Horizon 2020 research and innovation programme under grant agreement No 953219.

List of Figures

List of Tables

This project has received funding from the European Union's Horizon 2020 research and innovation programme under grant agreement No 953219.

List of Abbreviations

CM	Contour Method
CSC	Conical slit cell
DEC	Diffraction elastic constants
FEA	Finite element analysis
HD	Hole drilling
L-PBF	Laser powder bed fusion
LRI	Large-scale Research Infrastructure
LXRD	Laboratory X-ray Diffraction
ND	Neutron Diffraction
RS	Residual stress
SXRD	Synchrotron high energy X-ray Diffraction
SGV	Sampled gauge volume
TOF	Time of flight

This project has received funding from the European Union's Horizon 2020 research and innovation programme under grant agreement No 953219.

Table of Contents

Executive Summary

In order to develop a basis for comparing results from residual stress measurements, the basis of the main techniques has first been summarised in terms of their capabilities to capture specific components of an underlying internal stress state in metallic engineering components. An overview of each experimental methodology has been detailed, as it pertains to inter- and intra-technique comparison, alongside the predictions stemming from finite element analyses (FEA). This includes aspects of how stresses are averaged across the measured gauge volume, leading to best practices in comparing each technique's resolved stresses in terms of how results are conveyed, as well as how they are to be employed. Finally, an example of how this approach has been used to correlate the initial results obtained on one of the benchmark samples is presented. The purpose of this report is to provide the current best practice in comparing the results of the most prevalent residual stress measurement techniques, and how they might be employed to compare against FEA.

This project has received funding from the European Union's Horizon 2020 research and innovation programme under grant agreement No 953219.

Report on Implementation Process and Status of Deliverable

1. Introduction

There are many ways to infer the residual stresses (RS) that reside within metallic engineering components. All methods to some extent rely on capturing residual *strain* or change in shape of a component as an intermediate step, prior to applying elastic constants to obtain stress from these strains. The various techniques that can be employed are often limited on the basis of which stress components can be obtained. A stress at any point in an engineering body has 9 components, 6 of which are unique (Fig. 1). Some measurement techniques provide only some components by their nature, or by typical application. Further, the volume or region over which the stress is resolved can very different between each of the techniques.

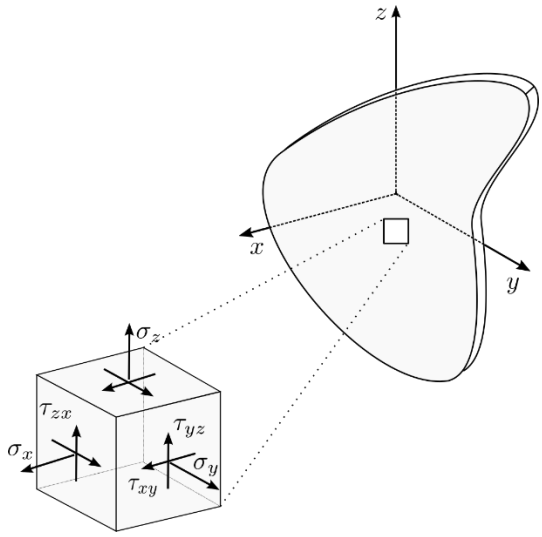

Technique	Available components
SXRD, ND	All are potentially viable, but typically three strain components are available: σ_x, σ_y and σ_z
LXRD, HD	Two near-surface main components and the resulting shear component: σ_x, σ_y and τ_{xy}, where $\sigma_z = 0$
CM	One complete component, and components relieved by application; one of: σ_x, σ_y or σ_z

Figure 1 – Depiction of the six unique stress components that describe a complete stress state in a body (Left). Strain components match the same convention. Techniques considered in EASI-STRESS with rendered components (Right).

This is why occasionally techniques are combined such that more components are accessed, this is made possible by the elastic nature of residual stresses. This can include a mix of both diffraction (SXRD, ND, LXRD) and strain-relief techniques (HD, CM). For example, those that are measured by a CM measurement, can then be measured with a complementary technique such as LXRD or HD. While the CM provides a full component, and parts of others, it permits access to a region within the bulk which would otherwise be inaccessible for LXRD/HD. The results of this sequential measurement approach can added in series to obtain all stress components at localised regions [1].

The outcome of any residual stress measurement campaign are the resulting stresses represented as scalar values and their locations, as well as the volume over which they have been averaged. These measurements can be employed to directly evaluate remediation techniques, *e.g.* post-weld heat treatments, or other residual stress modification approaches. However, they are most often employed to validate predictive computational models, with the prevailing type being FEA. These models are often developed with idealised material behaviour and physics with the aim of predicting the net effects of processing on the final residual stress state. The validation of these models adds dramatically to the utility and confidence of these models in application.

This project has received funding from the European Union's Horizon 2020 research and innovation programme under grant agreement No 953219.

Consequently, there is a need to develop procedures by which the results of different techniques or different measurements using the same technique can be compared. This could, for example, be a procedure to compare the results made using diffraction techniques (*e.g.* a series of ND measurements made with different instruments) as inter-technique. Alternatively, an intra-technique comparison would be made between a singular type of diffraction and strain-relief methods. The overriding assumption with regard to such inter-comparison studies (especially as some methods are destructive) is that multiple benchmark samples can be produced with identical residual stresses and underlying microstructure with a reproducibility higher than the required measurement uncertainty. These stress measurement techniques will be subsequently described within the context of comparison both within and between techniques, and further as applied to validating standard continuum-level finite element analyses. The aim of this report is to outline the various techniques available for residual stress measurement, supply methods for comparing results within the technique, between techniques and, finally, comparing them to predictions made with FEA.

2. Background

The various methodologies for measuring a residual stress state determine a particular stress component at a particular point in the artefact being considered. However, the specific value obtained as well as the error or confidence intervals may vary. This is partly because the physical basis underlying each methodology is quite different, but also because of sources of measurement error. Therefore, a measurement campaign that invokes two methods having very different underlying physics is very desirable in establishing confidence in measurement results.

FEA approaches are founded on the simulation of physical phenomena, which, if correctly realised, can be employed for optimisation and rapid prototyping. A major approach to determining the validity of a model is by comparing the residual stress state predicted versus that measured experimentally. Examples of validation of FEA in the literature often use a measured stress component at given points and compare these results directly to those predicted by FEA [2]. A FEA can provide spatially distributed fields, of which can be specific components of stresses, or equivalent stresses. These values are typically reported/displayed as values at particular points (nodes), which are then interpolated to provide a distribution within a particular component along a line or other path such that they can be compared with other measurements.

For comparison between different techniques, the following parameters must be considered:

i) The sampled gauge volume (SGV) over which the measurement was carried out.
ii) The positional accuracy of the respective measurement. For example, any errors or uncertainty in the position of the SGV within the subject part.
iii) Errors and uncertainty of the technique to resolve stress for the given metallic system, including variance in microstructure and resulting residual stresses.

These factors play an important role when comparing between measurement techniques, as well as when comparing to FEA results. For example, residual stress gradients finer than the resolution of some FEA results (or vice versa), and therefore some measurements (such as SXRD) may appear to not match those predicted. Similarly, ND results may be averaged over a larger volume of space than what is interpolated through an FEA model. Finally, the cause of a difference in the location of the maximum/minimum stresses may arise from positional error rather than a stress measurement error.

This project has received funding from the European Union's Horizon 2020 research and innovation programme under grant agreement No 953219.

The following is not a guide on how to perform the stress measurements themselves, but instead provides the current best practice in *comparing* the results of underlying techniques. This is first presented for comparing results obtained with the same technique (inter-technique) in the following section, followed by considerations for intra-technique, as well as comparison to FEA results.

3. Best practices in comparison

In order to establish best practices when compari**ng** RS measurement techniques, it is important to highlight that RS are classified over the length scale which they act. RS are commonly divided in three categories according to the length scale in which they act and self-equilibrate:

- Type I (macrostresses), acting over a length scale similar to the component under consideration or at least over a large number of grains;
- Type II (microstresses) vary over the grain size scale or at the interface of different phases; and
- Type III stresses vary over the length scales much less than a grain, e.g. those arising from dislocations and precipitates.

Type I RSs are the most widely characterised type in engineering components as this is the most important length scale as regards macroscopic failure phenomena such as fatigue and fracture. Destructive mechanical strain relief methods such as HD and CM typically operate at this length scale. Diffraction-based techniques which can be non-destructive involve aspects of Type II and III, directly measuring residual *strains*. Using these measured strains, a generalisation of Hooke's law determines the stresses in the corresponding directions for the corresponding domain. Stresses and strains of Type II are connected by single crystal elastic constants while the macroelastic constants (affecting a group of grains representative of the measured component) connect Type I strains and stresses. However, in order to ensure faithful comparison to FEA results, all techniques and their underlying length scales still require established procedures and best practice guidelines to ensure a correct characterization of residual stresses in position and magnitude. Best practices that are relevant to all techniques are as follows:

- Fiducial marks, provided by the sample supplier, are an asset not only for the correct positioning of the sample but to ensure the correct orientation. For example, in the case of samples produced by additive manufacturing, an incorrect identification of the starting and final printing faces (e.g. on a cubic shaped sample) can lead to incorrect correlation.
- For diffraction-based techniques, strategies needs to be employed to address microstructural variation. Diffraction techniques characterize the microstructure at atomic scale. This is not homogeneous because of local texture and other microstructural features Where possible, samples should be taken to have gauges larger than Type II variations, and many grains with different orientations should be examined. Where there may be sharp stress gradients, smaller gauge volumes and spatial increments between points can be employed. For strain-relief techniques, the same concept for small increments in measurement can also be applied in order to capture these sharp RS gradients.
- Aside from CM, all techniques will employ a SGV of some type. The use of a minimum representative SGV reduces the influence of the sample orientation with respect to measurement medium. When sharp RS profiles are present, it is recommended to use a small SGV dimension in that direction in order not to smooth them. However, this is not always possible and can only partially be avoided by using the minimum SGV length in the direction of the stress gradient.

This project has received funding from the European Union's Horizon 2020 research and innovation programme under grant agreement No 953219.

Based on these aspects, the specific underlying techniques will now be described, along with specifics germane to inter- and intra-technique comparisons.

3.1 LRI diffraction techniques

LRIs hosting high energy SXRD and ND techniques enable the measurement of RS within the bulk of the metallic parts. Residual stresses are averaged within a SGV and provide information of the different phases forming the material at different length scales. The basic physical principles are the same for all diffraction, as they rely on the crystal structure of the analysed phase to ascertain relative changes in the distance between parallel atomic planes oriented with their normal parallel to the scattering vector. The interplanar distances are calculated using the Bragg's law via the beam wavelength and the diffraction angle θ (Fig. 2).

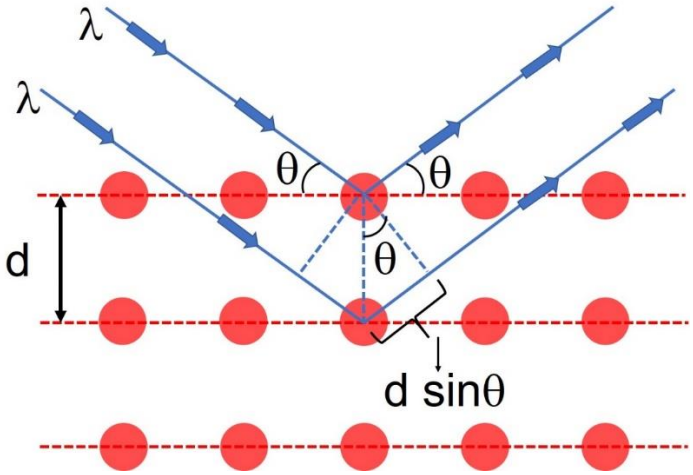

Figure 2 - Bragg's law connects the wavelength of the incident beam with the interplanar distance d and the diffraction angle θ.

From a practical standpoint, Type I stresses are calculated as the shift of the reflection peak of a certain atomic plane with respect to a stress-free sample. Problems arise when strains and stresses of different types have to be interrelated, *i.e.* Type I and II strains. When there are multiple phases of present, or when a single reflection is employed, then the measurement may be biased towards either an elastically stiffer or more compliant phase. The end result is that the Type II stresses do not average out for that particular phase or reflection. In such instances, Type II stresses must be taken into account if a reliable measure of the Type I stresses are to be obtained.

Further, the study of textured materials and the lack of knowledge of the single crystal elastic constants in some cases (as for directional solidified components such as those produced by additive manufacturing) can lead to large differences between RS calculated with diffraction techniques, those evaluated by strain-relief methods and those estimated by FEA. In addition to the above elastic anisotropy, plastic anisotropies can also mean that the peak shift recorded for a specific reflection may not be representative of the macrostress. It is therefore desirable to choose those planes weakly affected by intergranular strains. Finally, a correct determination of a stress-free reference is critical for confidence in RS measurement by diffraction. Different methodologies to accomplish this have been devised [3].

Although both techniques allow for the determination of a volume averaged RS acting in each phase, the decision to select one of the techniques depends primarily on three factors:

This project has received funding from the European Union's Horizon 2020 research and innovation programme under grant agreement No 953219.

a. Spatial resolution: local strain measurements require a small gauge volume and SXRD can be advantageous over ND. However, the typical SGV for synchrotrons is only small in 2 dimensions, for ND it is often cuboidal and of millimetric dimensions
b. Microstructure of the material: coarse grains require large gauge volumes to provide a more representative a more reliable assessment of Type I stresses. ND becomes in this case a preferred technique since the defined gauge volume (up to some hundred cubic millimetres) is typically much larger than for the SXRD (typically below 1 mm^2).
c. Sample dimensions: the use of SRXD is challenging when one or two dimensions are much larger than the others as this can lead to a long path length for the beam, owing to the low scattering angle associated with high X-ray energies. Under these conditions, ND has advantages compared to SXRD.

A final aspect that can influence the selection of one of the diffraction techniques is measurement time. With the third generation of synchrotron sources, acquisition times in the order of seconds are possible in some cases while ND generally requires upwards of minutes of acquisition time (even with the highest available neutron flux), although SXRD can become time consuming or indeed impractical for thicker cross-sections in high density metals. As a result, a balance in terms of the number of locations to be measured with any given campaign needs to be considered, as are specific aspects of SXRD and ND which will now be described.

a) SXRD

Synchrotron high energy X-ray diffraction can be divided into two main types, but are correlated in that they both employ X-ray energies with mean scattering angles of 2θ around 5-20°. The following describes key facets of each main type, with aspects that apply to correlation best practices:

- *Angle-dispersive synchrotron diffraction*: a monochromatic beam illuminates the sample providing information of the whole thickness. The diffracted beam cones are collected by a 2D detector with allows to obtain simultaneous information of the strains in a plane orthogonal to the beam. A depth-resolved strain analysis can be performed with a conical slit cell (CSC), which allows the gauge volume to be spatially defined [4]. A CSC comprises several concentric slits that are focused on a spot within the sample by their conical shape, while the focal distance is always constant. Depending on the phase to be analysed, the beam energy has to be tuned such the diffraction cones pass the slits. The gauge volume is elongated in the beam direction, smoothing stresses that can lead to differences with ND measurements or FEA predictions. The incident beam size usually varies between 50-200 µm in lateral dimensions. Standard slits are often employed for thin samples, whereby the beam penetrates the entire thickness, with the slits defining the area to be considered.
- *Energy-dispersive synchrotron diffraction*: photons diffract at different energies which are used to determine the atomic interplanar distances. Two point detectors can be used simultaneously to acquire strain information from two orthogonal directions at the same time [5]. Experiments can be performed either in transmission (bulk average strains) or in reflection (near surface strains). As for the case of the CSC, the gauge volume is elongated in the beam direction showing the same issue regarding RS smoothing.

b) ND

Neutron diffraction method for residual stress determination is characterized by the following advantages: extensive penetration into most engineering materials with a larger scattering angle of 2θ approximately 90° (Fig. 2) as compared to SXRD techniques. This allows a near-cubic gauge volume deep within the bulk of components. The gauge volume is defined by radial collimator

This project has received funding from the European Union's Horizon 2020 research and innovation programme under grant agreement No 953219.

and/or slits, with volume widths ranging from 0.5 mm to 10 mm. Depending on the type of beam being used, there are generally two types of neutron diffraction.

- *Monochromatic* neutron diffraction uses neutron beam, which wavelength (thus energy) has been pre-selected using a monochromator (usually a single crystal) before it is used to illuminate samples. The diffracted beam is commonly recorded using a position sensitive detector, which records a portion of the resulting Debye-Scherrer ring. The Bragg peak position is measured in 2θ, and the detector usually have a variable angular position. The changes in 2θ position with respect to stress-free reference values can be directly used to measure strain. Monochromatic neutron diffraction beamlines are usually located at continuous sources which generally offers higher time averaged monochromatic flux, therefore allowing faster counting time and/or higher spatial resolution and/or penetration depth. Since the resolution of the measurement is higher if the monochromator scattering angle has the opposite sign of the sample scattering angle, monochromatic ND generally gives one component of the strain in one measurement arrangement.
- *Time-of-flight* (TOF) neutron diffraction beamlines are naturally found at pulsed or spallation neutron sources. TOF neutron diffraction uses polychromatic or so-called 'white' neutron beam, which comprises a wide range of wavelengths (energies). As neutrons of different energy travel at different speeds, they arrive at the detector at different times. Time-resolved measurements are usually centred in a fixed angular position, *e.g.* at 2θ = 90°, recording multiple diffraction peaks from different crystallographic planes as a function of TOF and diffraction angle. The TOF of diffracted neutrons can be converted to the spacing of *d* (Fig. 2), which is then used for residual strain calculations. TOF instruments generally measure at least two perpendicular components of residual strains via the placement of two detectors in opposite scattering directions.

The most common sources of errors and misapplications in stress measurements using diffraction techniques are:

- Diffraction elastic constants (DEC)
- Texture
- Type III stresses
- Presence of different phases within a gauge volume

Normally, DEC and texture present the most significant impact on supplied measurements. The main reason is that isotropy assumptions are made in order to convert the measured strains into stresses. It is necessary to consider that oriented anisotropic single crystals (experimentally measured microscopic strains) are embedded in an oriented anisotropic medium. Therefore, it is prudent to employ multiple peaks where possible, such as those that are made available on TOF instruments. When dealing with textured materials or in directionally solidified materials (such as those additively manufactured) an isotropic hypothesis may not be not accurate. This is because standard approaches (*e.g.* Reuss and Voigt) cannot be used to calculate a DEC, and thus single crystal elastic constants are not known.

3.2 Laboratory-based techniques

There are three laboratory-based techniques for assessing residual stress that have been considered in EASI-STRESS based on the degree of commercial use. Two of which are local techniques (LXRD and HD) in that a localised region is subjected to measurement in the overall component. While the underlying basis for each are very different (diffraction versus strain relief), from a comparison perspective they are closely related in terms of the shape of the underlying gauge volume/area and

This project has received funding from the European Union's Horizon 2020 research and innovation programme under grant agreement No 953219.

stress components that can be obtained. The third method is the CM, which is a strain-relief method, but provides an entire cross-sectional map of a single stress component, as well as the portions of other components that are relieved by its application. These are subsequently described.

c) LXRD

For the laboratory X-ray diffraction (LXRD) method, a sample is illuminated by X-rays (much lower power than employed in synchrotron high energy X-ray diffraction) with wavelengths fixed by the nature of the tube used in the device (*e.g.* Cr, Mn, Cu, etc.). A Bragg peak position is set by the angular position of the detector. The nature of the sample dictates the wavelength and position of the detector in order to diffract a crystal plane with the highest meaningful signal. The EN 15305 standard provides recommendations on the setup on the basis of the subject metallic system. The gauge area is defined by the collimator (radial or sometimes rectangular) and the X-ray penetration is on the order of microns, rendering a near-planar SGV: it is effectively a gauge area as opposed to a volume. Measurements with this technique are made "in reflection" geometry and at large diffraction angles, to increase the sensitivity of the strain measurement and because low energy X-rays used do not have very high penetrative power. An acquisition is composed of several (minimum 7) acquisitions at different ψ angles (Fig. 3) in order to draw the curve strain in function of $\sin^2 \psi$. Typically, this is accomplished with ψ oscillations of ± 6°. A similar approach with a different arrangement of detector and X-ray illumination can be applied employing a function of cosα (Fig. 3). This technique has the advantage of being fairly rapid with appropriate sample preparation.

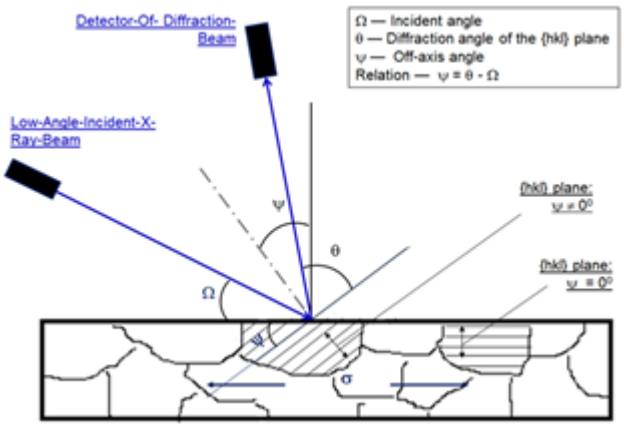

Figure 3 – Bragg's law connecting the wavelength of the incident beam with the interplanar distance d and the diffraction angle θ. Oscillations about ψ and α are employed to acquire an adequate signal for residual strain measurements.

The most common sources of error are the same as for the previously described diffraction techniques (Section 3.1). This includes uncertainties in DECs, texture (including grain size effects), Type III stresses, and the presence of multiple phases or composition/content gradients. These errors can impact the stress calculation (Fig. 4). Often, surface roughness can exacerbate these types of errors, and therefore sample preparation will sometimes require electrochemical etching. This typically removes approximately 50-100 µm from the subject surface. It is possible to obtain a residual stress profile in depth by successive applications of electrochemical etching.

This project has received funding from the European Union's Horizon 2020 research and innovation programme under grant agreement No 953219.

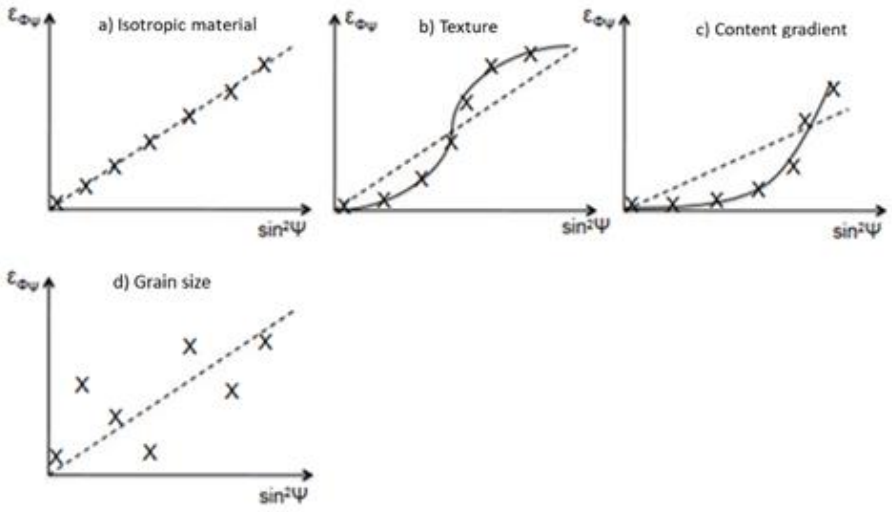

Figure 4 : Different $\sin^2\psi$ curves on materials with different microstructures, with departures from an idealised isotropic material response. The dotted line shows the curve calculated from experimental points to calculate the residual stress with variations from this idealised isotropic response.

d) HD

Like LXRD, Hole drilling (HD) can measure the 3 in-plane stress components, however with larger gauge volumes/areas. It is a much more rapid way to probe the variation of this in-plane stress as a function of depth when compared to LXRD, and is effective to a depth similar to the diameter of the hole imposed. Similar to LXRD, there is a recognised standard for application, ASTM E837. As shown in Fig. 5, The technique relies on measuring how surface strain changes as material is mechanically removed by high-speed drilling in small depth increments [6]. Being a purely mechanical measurement technique, the potential sources of error are very different from those inherent in LXRD; it is insensitive to Type II and III stresses, but other sources of error are important including cutting plasticity and potential gauging errors.

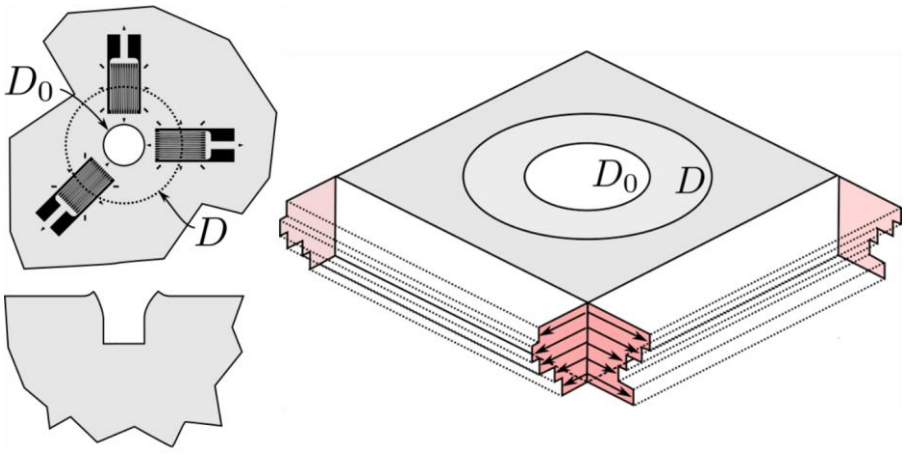

Figure 5 - Schematic representation of a hole drilling measurement. A hole is with diameter D_0 is drilled to a set depth, while the change in strain occurring about diameter D is monitored by strain gauging (left). Successive applications can obtain residual stress profiles in depth (right).

Variations in the technique include the underlying drilling technology (high speed machining versus electro-discharge machining), as well as how the surface strains are captured. Surface strains are either recorded with strain transducers (Fig. 5) on a rosette whose resistivity changes as it deforms,

This project has received funding from the European Union's Horizon 2020 research and innovation programme under grant agreement No 953219.

or by optical techniques – digital image correlation, electronic speckle pattern interferometry or Moiré interferometry.

e) CM

The contour method (CM) is a laboratory-based, destructive strain relief method which involves cutting a component into two or more sections, and then employing high resolution surface profiling to measure the deviations from flatness of the cut faces (*i.e.* their surface contour) induced by stress relaxation [7]. The surface contour is then numerically processed (usually by FEA) to infer the stress required to form the deflected surface, given the relevant elastic moduli. Cutting is typically realised by electrodischarge machining, whereby an electrically excited wire is moved through the part to be measured. The result is a two-dimensional map of a complete stress component normal to the cutting plane, along with the other components of stresses that were relieved due to the cut. This is what differentiates the CM from other laboratory-based local techniques previously described. Instead of singular values of stresses which pertain to a localised regions or volumes within a part to be measured, a complete map of a stress component is obtained across some cross-section.

The point density of individually resolved stress values is dependent on a variety of factors, including underlying resolution of the metrology method used, and the numerical technique for calculating stresses from this data. While there is not a recognised standard, there is a best practice guideline aimed at achieving repeatability between practitioners [8], with some efforts to compare results from different practitioners only now emerging [9].

For correlation to other techniques, the best approach is to employ a standardised way of reporting results or the provision of the underlying FEA calculation employed to obtain stresses from the surface deflection measurements. However, even in the latter case, it is best practice to select coordinate axes relative to the component as shown in Fig. 6. By orienting the x-axis along the cutting path, and the y-axis along the cutting direction, additional information that assists with reproducibility efforts are built into the measurement report. A ‘full’ contour result consists of locations of nodes lying on the cut face, and the stress components at each node. Alternatively, many FEA post-processors are able to interpolate points along lines to render a direct correlation to other techniques; this too could be realised by linear interpolation of stress values from the stress and location data of nodes on the cut face.

The error or repeatability in the contour method is different than that typified by the preceding measurement types as there are multiple sources of error, and these could be spatially biased depending on cutting protocol or analysis decisions. For example, in Fig. 6, the peak resolved CM stresses recorded for the benchmark weld when compared to neutron diffraction are smaller and somewhat shifted. This is because of plasticity occurring during the cut, resulting in an inelastic redistribution of residual stress.

This project has received funding from the European Union’s Horizon 2020 research and innovation programme under grant agreement No 953219.

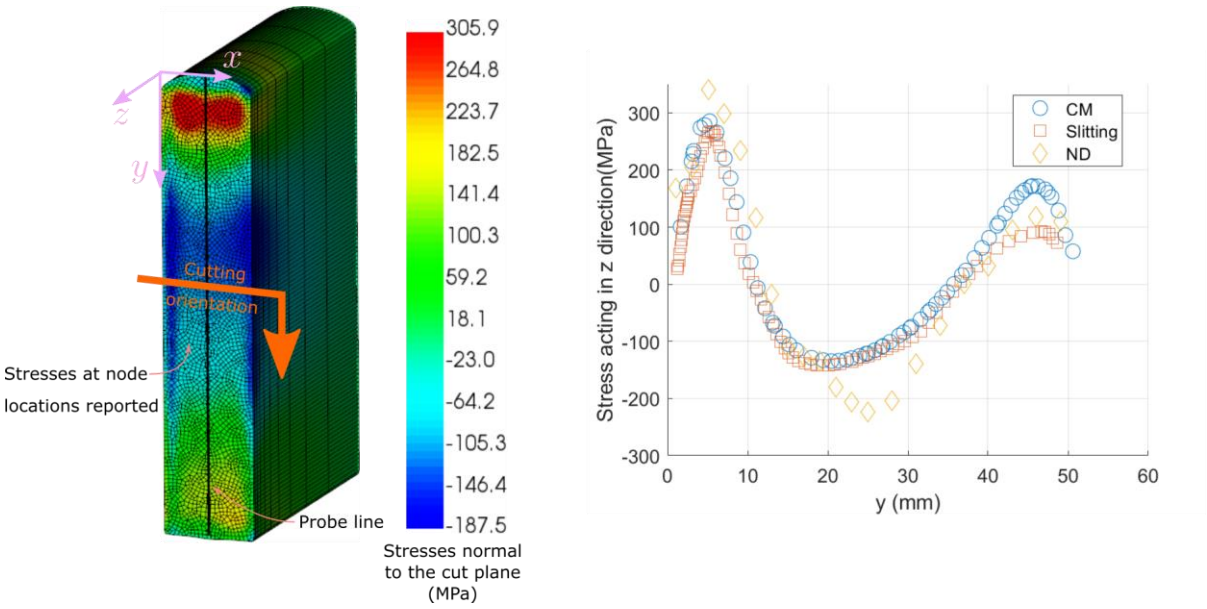

Figure 6 - An example of a contour measurement performed on a historical benchmark AISI 316H autogenously edge-welded beam for residual stress measurements [10] *which precedes EASI-STRESS. Annotations depict prescribed reporting of stresses and locations. Note that ND results should provide both position and resolved stress error envelopes, which were not available from the published results.*

In summary, both LXRD and HD are near surface-based techniques, that only measure the in-plane stress components (Fig. 1). This is because in all instances, the out-of-plane stress components are effectively taken as zero, and it is therefore necessary to couple this technique with other stress measurements techniques to obtain a complete stress tensor. In the laboratory, these methods can be coupled with CM results in order to provide a complete set of stress components at local regions of interest.

4. Inter-technique and FEA comparison

For the purposes of correlation between techniques, a standardised data reporting template that accounts for the different underlying basis for each measurement has been proposed. This proposed template coincides and agrees with the data reporting format described in EASI-STRESS D5.1 intended solely for inter-technique reporting. As described above, each technique considered encompasses different aspects which may affect the final results, and the proposed template allows flexibility while communicating these, as shown schematically in Fig. 7.

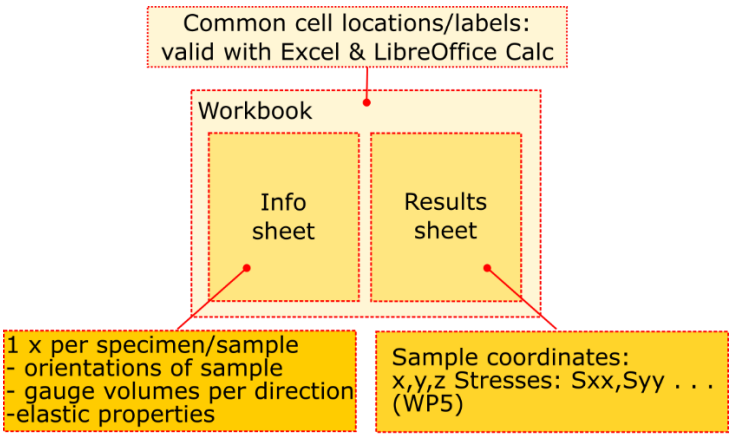

Figure 7 - Workbook-based format suitable for reporting inter- and intra-technique residual stress measurements.

This project has received funding from the European Union's Horizon 2020 research and innovation programme under grant agreement No 953219.

This format was selected on the basis of accessibility and ease of access by all stakeholders, whilst maintaining the formatting required specifically by industrial stakeholders during the course of WP5, *i.e.* end-users of residual stress measurements. With the above format, the effect of specific aspects of the measurement can be clearly conveyed. For example, different gauge volume orientations can be clearly communicated, and can be correlated to the final outcome in a particular orientation (see items a-c in Section 3.1). Effective comparative geometries and approaches are described subsequently, followed by an example of how this approach has been applied to date on a benchmark sample.

4.1 Effective comparison geometries

As has been described in the preceding sections, the effective volumes or areas over which different measurement techniques can be applied can be quite different. Therefore, there is a need to describe specific treatments of results as they compare to each other (inter-technique) as well as how they can be compared to FEA predictions. Historically, most measurements of residual stress are expressed as single values at a given point. However, the reality is that there are different SGVs associated with each technique, and stresses are averaged over the extent of this volume as described in Section 2. For example, a ND campaign may produce measurements with SGVs of different sizes along different directions, which may encompass a large gradient. This could result in over-averaging of stresses in the longer dimensions of the SGV. A single value obtained from an FEA compared to this value will not take this into account. Therefore, it is prudent to apply a pragmatic approach to the geometries and locations which are to be compared. These suggestions are summarised briefly in Table 1.

Table 1 - Overview of suggested geometric considerations when considering inter-technique and FEA comparisons of residual stress measurements and predictions.

Technique	Geometric boundaries stresses are averaged over	Inter-technique comparison	Advanced treatment of FEA results**
SXRD, ND	Spherical* volume with radius equal to the largest dimension of the SGV.	Direct comparison between geometric boundaries for HD and LXRD, resampled CM results.	Averaged stresses at either nodes or integration points lying in geometric boundaries.
LXRD, HD	Equivalent circular area equal to illumination dimensions for LXRD or D_0 for HD.	Direct comparison between geometric boundaries for SXRD and ND, resampled CM results.	Averaged stresses found in equivalent circular areas of measurement.
CM	Point-based interpolation from CM FEA calculation.	Averaged stresses at nodes or integration points lying within** respective geometric boundaries of subject technique.	Direct comparison between CM and subject FEA employing points interpolated between nodes or integration points

*For cases of extreme differences in SGV dimensions, an ellipsoid can be considered. **If the underlying FEA has a fine enough discretisation to permit these approaches to be taken.

Of course, this advanced type of approach can be neglected in favour of applying the practice commonly applied in the literature, which considers stresses obtained as scalar values applicable to a single point located at the centroid of the relevant SGV. This is particularly the case when

This project has received funding from the European Union's Horizon 2020 research and innovation programme under grant agreement No 953219.

comparing results from a spatially coarse FEA or it is known that the length scale of the residual stresses far exceeds any given dimension of the SGV.

4.2 Exemplar comparison in a benchmark sample

An example how the data format described in Fig. 7 has been employed and a first attempt at comparing measurements to FEA results is described below for the additively manufactured benchmark samples. A first comparison of an equivalent stress in this laser powder bed fusion (L-PBF) arch sample has been accomplished between the experimental stresses measured by energy-dispersive diffraction in transmission mode at the Hereon LRI and a purely mechanical FEA performed with the Amphyon software at industrial partner ArcelorMittal. Stresses were compared at as-built state with the sample still attached at the build plate to measure the real stresses coming from the manufacturing process. This process has been described in detail in D2.1. In total. five different scanning lines were measured at Hereon, which are labelled as Line 1 – Line 5 in Fig. 8.

An equivalent stress based on a Von Mises formulation was generated by measuring three directions at each point and assuming that the three measured directions were equivalent to the principal stresses. Therefore, it is expected that there will be a deviation from the captured equivalent stress at each point as compared to actual Von Mises as predicted by the FEA. This difference will be studied in the future by measuring 6 directions at each point and capture the full stress tensor at each point. Regardless, good agreement was found across the centreline of the components.

Stress symmetry in the sample was studied by measuring Lines 3 and 4 (Figure 8Fig. 8) where both pillars of the arch were measured from the bottom to the top. Interestingly, results were very symmetric, showing similar stress trends, albeit with the simulation showing significantly higher stresses throughout.

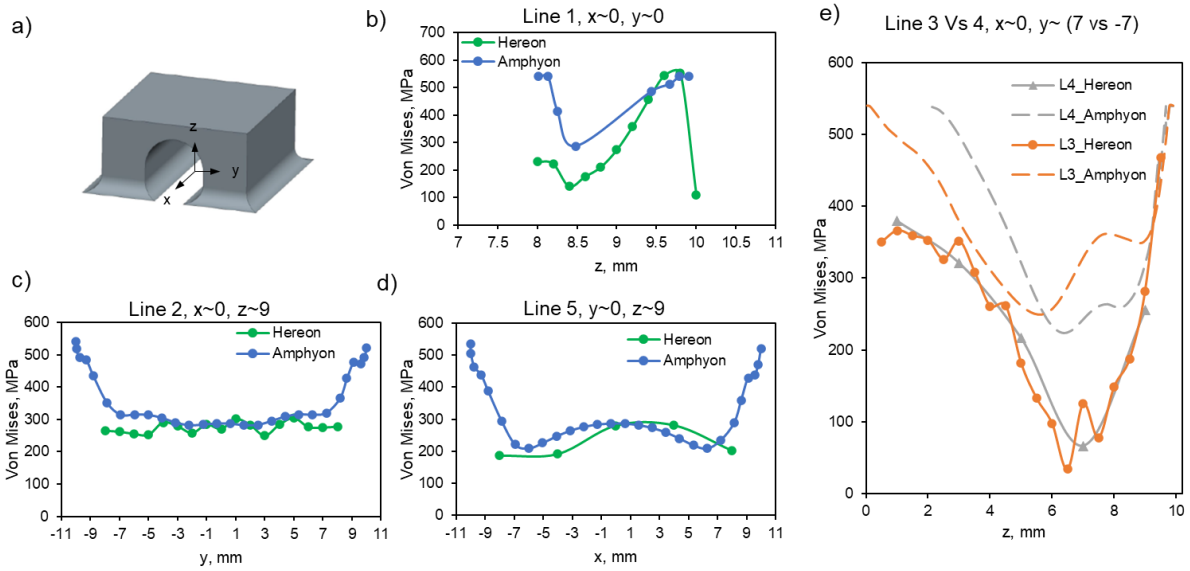

Figure 8 a) Depiction of the WP2 additively manufactured arch sample with the origin reference located at the centre of the bottom xy plane. Assessment of the Von Mises stresses calculated by Amphyon model (in blue) and measured by diffraction at Hereon (in green) at different scan lines: b) Line 1: (0, 0, z), c) Line 2: (0, y, 9) and d) Line 5: (x, 0, 9). Two vertical lines to compare stress symmetry were compared at e) Line 3: (0, 7, z) in orange and Line 4: (0, -7, z) in grey. Note than dashed lines correspond to the results obtained by FEA.

The first results from mechanical simulation are not very far from the experimental measurements. There are appreciable differences in the obtained numerical values, however in-plane stresses are

This project has received funding from the European Union's Horizon 2020 research and innovation programme under grant agreement No 953219.

well predicted (Fig. 8 (c) and (d)). In addition, stress tendency at each scan direction is well predicted in the simulations.

Moreover, new simulations using more sophisticated software are in progress, for which tensile properties at different temperatures are being measured to improve the constitutive equations. In this way, it is expected that residual stresses simulations for additive manufacturing will be improved and more accurate results will be achieved. Taking also into account that more accurate Von Mises stresses can be calculated by measuring the full tensor, it can be concluded that the results of this first approach are very promising, with room for experimental and simulation improvement with the currently available tools in order to define best practices for measuring and comparing residual stresses in additive manufacturing components.

5. Summary

This report has provided an overview of the capabilities of each residual stress measurement technique that is currently available. Further, outlining the applications of each technique has identified aspects that can be critical to consider when comparing results between them, and for the purposes of comparing/validating the results of FEA predictions. Work to date has carefully considered these factors. It has informed the development of a standardised method for reporting the results of measurement campaigns, as well as a more advanced technique for comparing results between techniques and with those stemming from an FEA. This latter point has been exemplified by work to date in measurement and comparison of the additively manufactured benchmark sample. Participants in this WP will continue to realise further results with more techniques, and it is expected that the approaches suggested here will be proven out with more data from the full range of benchmark specimens.

This project has received funding from the European Union's Horizon 2020 research and innovation programme under grant agreement No 953219.

6. References

[1] P. Pagliaro, M. B. Prime, H. Swenson, and B. Zuccarello, "Measuring Multiple Residual-Stress Components using the Contour Method and Multiple Cuts," *Exp. Mech.*, vol. 50, no. 2, pp. 187–194, Aug. 2009, doi: 10.1007/s11340-009-9280-3.

[2] M. C. Smith, A. C. Smith, C. Ohms, and R. C. Wimpory, "The NeT Task Group 4 residual stress measurement and analysis round robin on a three-pass slot-welded plate specimen," *Int. J. Press. Vessel. Pip.*, vol. 164, pp. 3–21, 2018, doi: https://doi.org/10.1016/j.ijpvp.2017.09.003.

[3] P. J. Withers, M. Preuss, A. Steuwer, and J. W. L. Pang, "Methods for obtaining the strain-free lattice parameter when using diffraction to determine residual stress," *J. Appl. Crystallogr.*, vol. 40, no. 5, pp. 891–904, Oct. 2007, doi: 10.1107/S0021889807030269.

[4] P. Staron *et al.*, "Depth-Resolved Residual Stress Analysis with Conical Slits for High-Energy X-Rays," in *Mechanical Stress Evaluation by Neutrons and Synchrotron Radiation VI*, 2014, vol. 772, pp. 3–7, doi: 10.4028/www.scientific.net/MSF.772.3.

[5] A. Steuwer, J. R. Santisteban, M. Turski, P. J. Withers, and T. Buslaps, "High-resolution strain mapping in bulk samples using full-profile analysis of energy-dispersive synchrotron X-ray diffraction data," *J. Appl. Crystallogr.*, vol. 37, no. 6, pp. 883–889, Dec. 2004, doi: 10.1107/S0021889804023349.

[6] G. S. Schajer and P. S. Whitehead, "Hole-drilling method for measuring residual stresses," *Synth. SEM Lect. Exp. Mech.*, vol. 1, no. 1, pp. 1–186, 2018.

[7] M. J. Roy, N. Stoyanov, R. J. Moat, and P. J. Withers, "pyCM: An open-source computational framework for residual stress analysis employing the Contour Method," *SoftwareX*, vol. 11, p. 100458, 2020, doi: https://doi.org/10.1016/j.softx.2020.100458.

[8] F. Hosseinzadeh, J. Kowal, and P. J. Bouchard, "Towards good practice guidelines for the contour method of residual stress measurement," *J. Eng.*, Jan. 2014, [Online]. Available: http://digital-library.theiet.org/content/journals/10.1049/joe.2014.0134.

[9] C. R. D'Elia *et al.*, "Interlaboratory Reproducibility of Contour Method Data Analysis and Residual Stress Calculation," *Exp. Mech.*, vol. 60, no. 6, pp. 833–845, 2020, doi: 10.1007/s11340-020-00599-0.

[10] F. Hosseinzadeh, M. Burak Toparli, and P. John Bouchard, "Slitting and Contour Method Residual Stress Measurements in an Edge Welded Beam," *J. Press. Vessel Technol.*, vol. 134, no. 1, 2011, doi: 10.1115/1.4004626.

This project has received funding from the European Union's Horizon 2020 research and innovation programme under grant agreement No 953219.